Reconfigurable Deployable Polyhedral Mechanism Based on Extended Parallelogram Mechanism

Ruiming Li[1], Yan'an Yao[1,*], Xianwen Kong[2,*]

[1] *School of Mechanical, Electronic and Control Engineering, Beijing Jiaotong University, Beijing, 100044, China, E-mail: 08116302@bjtu.edu.cn.*

[1,*] *School of Mechanical, Electronic and Control Engineering, Beijing Jiaotong University, Beijing, 100044, China, E-mail:yayao@bjtu.edu.cn.*

[2,*] *School of Engineering and Physical Sciences, Heriot-Watt University, Edinburgh, EH14 4AS, UK, E-mail: X.Kong@hw.ac.uk.*

Abstract: This paper dealt with the construction of a novel class of reconfigurable deployable polyhedral mechanisms (RDPMs). A parallelograms mechanism was designed by considering layers of links and size of revolute joints, and extended parallelogram mechanisms (EPaM) were constructed for the first time by inserting angulated elements and scissor-like elements into the parallelogram mechanism. The detailed parameters and magnification ratios of two kinds of EPaMs were calculated. A method was then proposed for constructing RDPMs based on EPaMs. The proposed method can provide more modular linkages for RDPMs, and all polyhedra constituted by regular polygons can be used to construct RDPMs. The obtained RDPMs can be reassembled by increasing or decreasing the number of basic elements to change the sizes beyond their deployment capacity. A prototype of reconfigurable deployable hexahedral mechanism based on EPaMs was fabricated to verify the feasibility of this class of RDPMs, and three reconfigurable deployable hexahedral mechanisms in three sizes based on the prototype were reassembled and tested.

Keywords: Reconfigurable Mechanism, Deployable Mechanism, Extended Parallelogram Mechanism, Angulated element, Polyhedron

Nomenclature

RDPM	reconfigurable deployable polyhedral mechanisms
AEs	angulated elements
SEs	scissor-like elements
DSCM	double slider-crank mechanism
SSCM	single slider crank mechanism
PaM	parallelograms mechanism
EPaM	extended parallelogram mechanisms
RDHM	reconfigurable deployable hexahedral mechanism
l	side length of a polygon constructed by EPaM
l_{max}	maximum value of side length of a polygon constructed by EPaM
l_{min}	minimum value of side length of a polygon constructed by EPaM
L	distance between two adjacent revolute joints
GE_{max}	maximum value of the length of the link GE
OE_{max}	maximum distance between points O and E
OE_{Dmin}	minimum distance between points O and E in the DSCM mode
OE_{Smin}	minimum distance between points O and E in the SSCM mode

OG_{max}	maximum value of the length of the crank OG
R_{Dm}	magnification ratio of EPaMs in the DSCM mode
R_{Dm}^{O}	magnification ratio of RDPMs in the DSCM mode
R_{m}^{O}	magnification ratio of RDPMs
R_{Sm}	magnification ratio of EPaMs in the SSCM mode
R_{Sm}^{O}	magnification ratio of RDPMs in the SSCM mode
w	diameter of revolute joints
θ	interior angle of the polygon constructed EPaM
γ	included angle of the AE
γ_1	included angle of AE-1 in 2-AEs-EPaM
γ_2	included angle of AE-2 in 2-AEs-EPaM

1 Introduction

Deployable mechanisms, which are also known as deployable structures [1, 2], have received much attention from many researchers due to their potential application in architecture and space exploration. The general design method of deployable mechanisms based on scissor-like was pioneered by Pienro's work on the movable theatre [3] and was further developed by Escrig [4]. Deployable mechanisms can be in different geometric shapes such as plane [5], cylinder [6], prism [7] and polyhedron [8-18] etc. Recently deployable polyhedral mechanisms (DPM) preserving polyhedral shape during deployment have become one of the research focuses in deployable mechanisms. They are usually synthesized by inserting modular linkages into the faces of regular or irregular polyhedra (platonic polyhedrons, semiregular polyhedrons and even Johnson solids). Hoberman [8] constructed the Hoberman sphere and other inventions based on angulated element, which later was generalized by You and Pellegrino [9]. Wohlhart [10-12] synthesized zig-zag linkages, regular polyhedral linkages and twisting towers using Nuremberg scissors, planar link groups and double rotor connecters respectively. Wei et al. [13] proposed a single-plane-symmetric 8-bar linkage and synthesized a class of semiregular and Johnson DPMs. Kiper et al. [14] proposed a synthesis method for constructing Fulleroid-like DPMs base on the principle of Cardan motion. Kovács et al. [15] constructed expendable polyhedral structures to imitate the reversible expansion of viruses. Wei et al. [16] created a class of expandable structure for spatial objects which were constructed by connecting a series of parallelogram mechanisms. Gosselin and Gagnon-Lachance [17] constructed a new type of one-DOF expandable mechanism using one-DOF planar linkages and spherical joints, and they also carried out detailed mechanical design to reach high expansion ratio [18].

In order to increase the adaptability of DPM as parallel manipulators with multiple operation modes [19, 20], several reconfigurable deployable polyhedral mechanisms (RDPM) have been proposed recently. The term "deployable" refers to the scaling ability of the mechanisms. When a deployable mechanism is defined as "reconfigurable", the mechanism normally can change assembly modes or motion modes during operation without disassembly and reassembly. Wei and Dai [21] constructed a group of reconfigurable deployable platonic mechanisms using variable revolute joints, which can transform themselves between Fulleroid-like linkage type and the star-transformer linkage type. Li et al. [22, 23] proposed a method of constructing reconfigurable deployable platonic mechanisms based on reconfigurable angulated elements. Especially, Wohlhart [24] constructed a class of reconfigurable mechanisms named "Cupola Linkages" based on double shields modules. Double shields modules can switch between double slider crank mechanisms and single slider crank

mechanism, so that the “Cupola Linkages” is reconfigurable. However, the “Cupola Linkages” lacks of detailed mechanical design and expandability. In this paper, we designed parallelograms mechanism (PaM) by considering layers of links and size of revolute joints, and proposed extended parallelograms mechanism (EPaM) by inserting angulated elements (AEs) and scissor-like elements (SEs) into PaM. A family of RDPMs based on PaM and EPaM was synthesized. The proposed method can provide more modular linkages for RDPMs and increase the expandability of the RDPMs. The expandability mainly consists of two aspects: (1) We can design RDPMs using different modular linkages; (2) We can reassemble RDPMs by increasing or decreasing the number of AEs and SEs to change the size beyond their deployment capacity. The obtained RDPMs can have bigger magnification ratios and can be reassembled to different sizes to meet a variety of application requirements.

This paper is organized as follows: In section 2, an n-parallelograms mechanism is built by arranging double slider crank mechanism circumferentially. Two kinds of extended parallelogram mechanisms with AEs and SEs are constructed in section 3. A method for constructing EPaM-based RDPM is illustrated in section 4. In section 5, a prototype is fabricated to verify the proposed method. Section 6 concludes the paper.

2 n-parallelograms mechanism

In this section, *n*-parallelograms mechanism was designed and investigated. A double slider-crank mechanism (DSCM) consists of two identical cranks, two identical links and a slider (Fig. 1(a)). When two cranks coincide with each other, the DSCM switches to a single slider crank mechanism (SSCM), as shown in Fig. 1(b). An n-parallelograms mechanism (n-PaM) can be constructed using n DSCMs as follows. Firstly, we evenly arrange n DSCMs circumferentially. Secondly, merger the n cranks in the same layer to form a star-like central link with n branches. Thirdly, eliminate the sliders and keep the two adjacent links of each slider connected by a revolute joint. Finally we get an n-PaM around a circle. The diagram of n-PaM is shown in Fig. 1(c), and include angle between two adjacent branches of central link can be calculated by 360°/*n*, where *n* denotes the number of PaM. 6-PaM as an example is shown in Fig. 1(d), and it has two central links with 6 branches and 12 edge links.

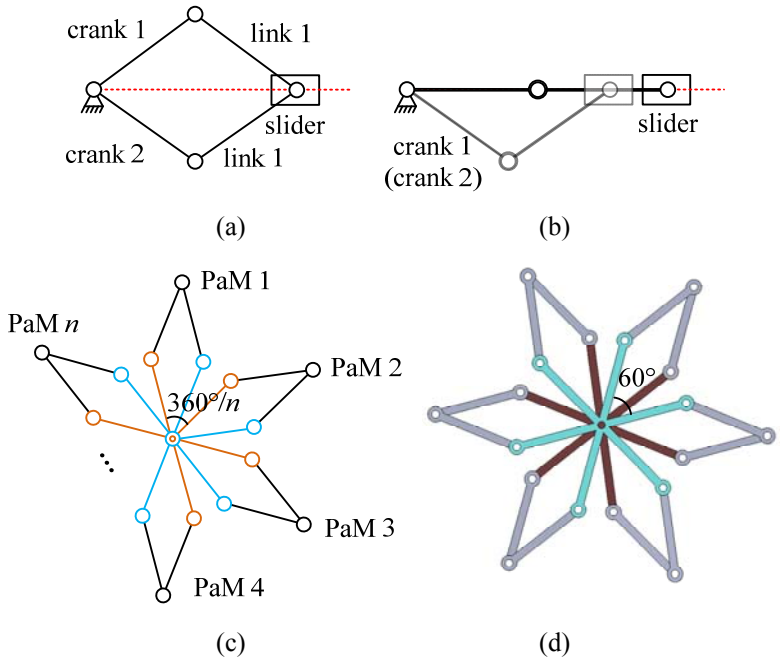

Fig. 1 Double slider crank mechanism and n-PaM: (a) DSCM, (b) SSCM, (c) n-PaM, (d) 6-PaM.

The obtained n-PaM theoretically can switch between two 1-DOF (degree-of-freedom) modes: DSCM mode and SSCM mode. However, the reconfigurable function of n-PaM highly depends on its mechanical structure. According to the diagram of n-PaM in Fig. 1(c), a 4-PaM consists of two star-like central links and eight edge links. If all the links are arranged into two layers (Fig. 2(a)), 4-PaM is still movable but cannot achieve reconfiguration due to physical interference. As shown in Fig. 2(b), when the links are arranged into four layers with two central links lying on the first and fourth layers, 4-PaM is movable and reconfigurable. Figures 2(c)-2(e) are the top view of Fig. 2(b). The centers of joints *a*, *b*, *c* and *d* slide along axis *ac* and axis *bd*, respectively. In DSCM mode, two central links rotate in the opposite direction, while in SSCM mode, two central links rotate in the same direction.

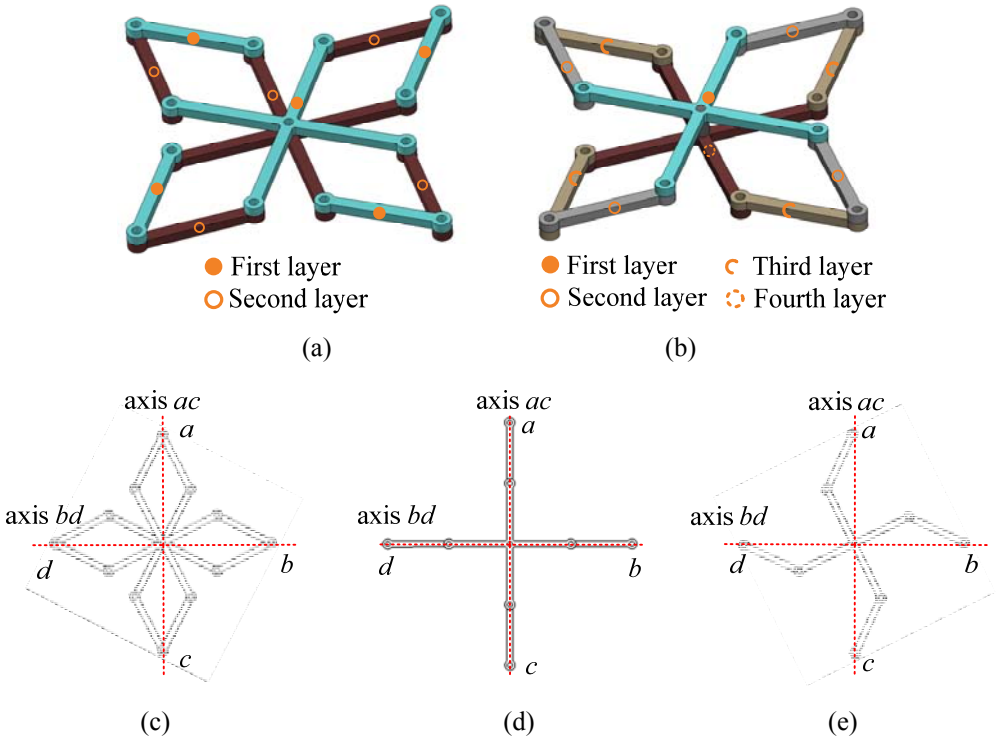

Fig. 2 4-parallelograms mechanism: (a) DSCM mode, (b) transition configuration, (c) SSCM mode.

By inserting 4-PaM into six quadrilateral faces, a reconfigurable deployable hexahedral mechanism (RDHM) can be constructed. The RDHM herein and in Section 3 will be used as an example to compare different parallelogram mechanisms. The detailed construction process will be introduced in Section 4. The RDHM can switch to DSCM mode or SSCM mode from the transition configuration, as shown in Fig. 3.

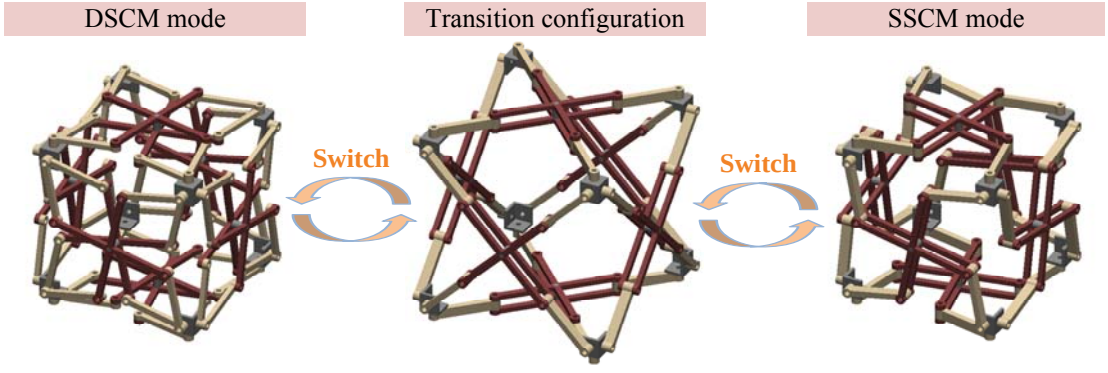

Fig. 3 Reconfigurable deployable hexahedral mechanism based on 4-PaM.

3 Extended Parallelogram Mechanism

To increase SEs'/AEs' number and overall size of a PaM, this section deals with extended parallelogram mechanisms (EPaM) by inserting extra elements into a PaM. Two kinds of basic elements are shown in Fig. 4, the parameters of SE satisfy: $as=bs$, $cs=ds$ and $\gamma_1=\gamma_2=\pi$, and the parameters of AE satisfy: $as=bs$, $cs=ds$ and $\gamma_1=\gamma_2\neq\pi$. Although SEs [10, 23] are usually used to increase the size or magnification ratio of deployable mechanisms, they do not meet the requirement for reconfiguration, because the mechanism will degenerate into an n-*R* serial mechanism in the transition configuration. SEs and AEs play different roles in construction of EPaM. SEs are for increasing the size while AEs are for achieving reconfiguration. The number of SEs depends on the size of EPaM, while normally one or two AEs should be enough for reconfiguration. Therefore in this paper EPaMs can be divided into two categories: EPaM with one AE (1-AE-EPaM) and EPaM with two AEs (2-AEs-EPaM).

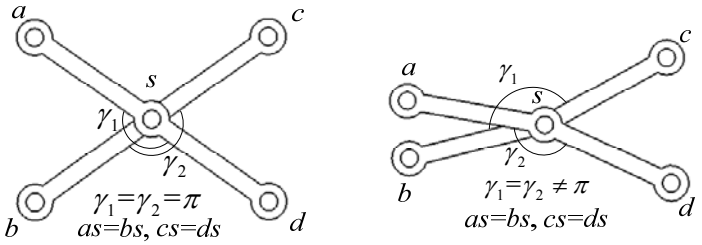

(a) (b)

Fig. 4 Basic element: (a) Scissor-like element, (b) angulated element.

3.1 1-AE-EPaM

1-AE-EPaM (Fig. 5(a)) consists of two central links, two edge links and a pair of AE, and the structure design is shown in Fig. 5(b). The mechanism has four layers to ensure that the joints *A* and *B* coincide with each other at transition configuration I (Fig. 5(c)) or joints *C* and *D* coincide with each other at transition configuration II (Fig. 5(d)). The mechanism may switch to the SSCM mode I (Fig. 5(e)) from transition configuration I, in which mode the mechanism has a shorter crank and a longer link. The mechanism may also switch to the SSCM mode II (Fig. 5(f)) from transition configuration II, in which mode the mechanism has a longer crank and a shorter link. In both SSCM mode I and SSCM mode II, point *O* is fixed to ground, and point *E* is assumed to slide along virtual axis *OE*. The mechanism can also deploy in DSCM mode I (Fig. 5(g)) and DSCM mode II (Fig. 5(h)). In DSCM mode I, $\angle ASB$ is smaller than $\angle CSD$, while in DSCM mode II, $\angle ASB$ is larger than $\angle CSD$. To maximize the magnification ratio, the link lengths satisfy the following conditions:

$$OA=OB=AS=BS=CS=DS=CE=DE=L \tag{1}$$

where *L* denotes the distance between any two adjacent revolute joints.

For the deployable mechanism, the bearings will normally be installed in the revolute joints, the external diameter of the revolute joint is wider than rest parts of the elements, so the interference happens between two adjacent revolute joints. Assume that joints C and D be tangent to each other when joints A and B coincide, as shown in Fig. 5(e). The included angle of the AE can be calculated by Eq. (2). Due to the symmetry and special parameters of 1-AE-EPaM, joints A and B also are tangent to each other when joints C and D coincide, as shown in Fig. 5(f).

$$\gamma=\pi-\arcsin(\frac{w}{2L}) \tag{2}$$

where w denotes the external diameter of the revolute joint.

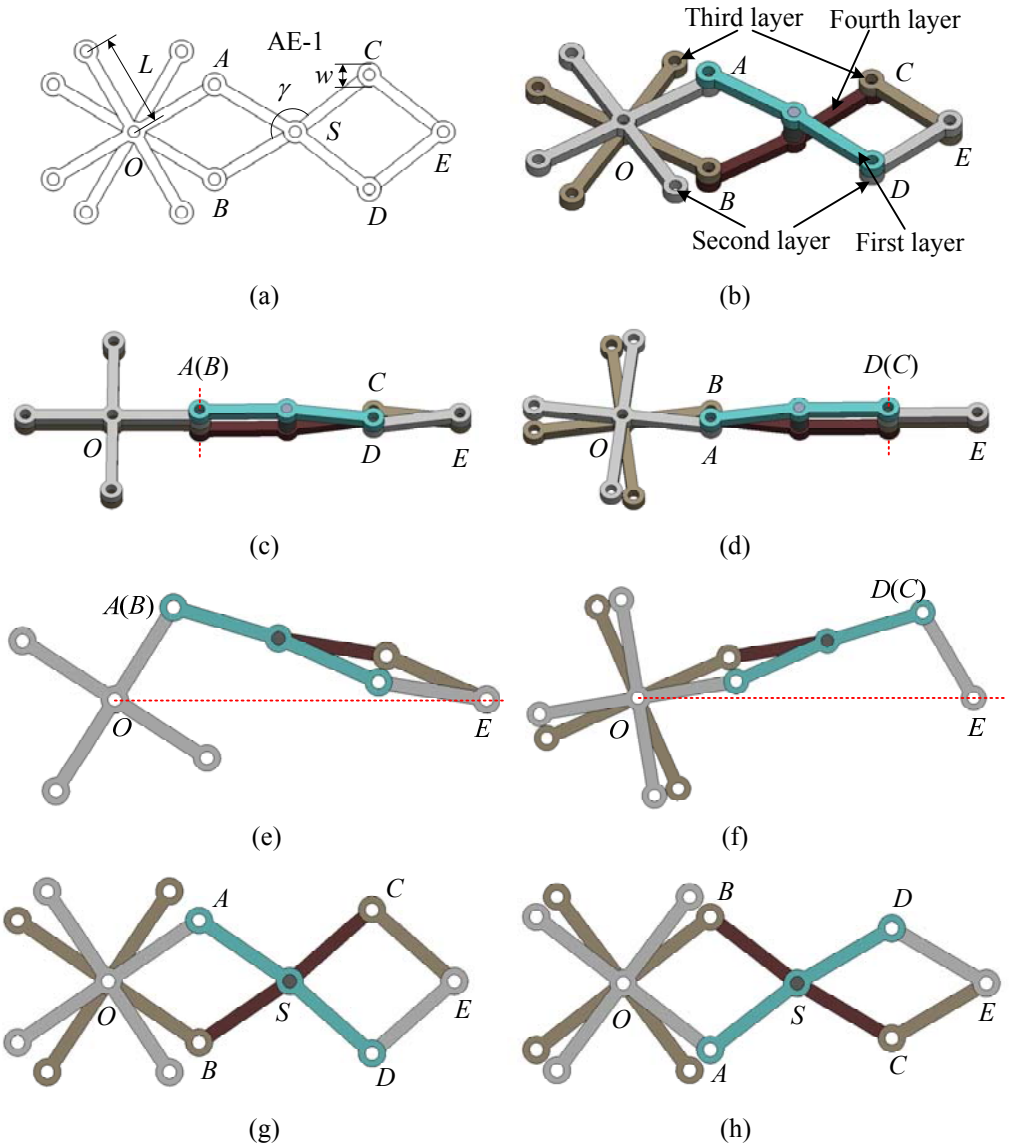

Fig. 5 1-AE-EPaM: (a) Diagram, (b) structure design, (c) transition configuration I, (d) transition configuration II, (e) SSCM mode I, (f) SSCM mode II, (g) DSCM mode I, (h) DSCM mode II.

A reconfigurable square can be constructed by evenly arranging four 1-AE-EPaMs circumferentially. By inserting the constructed reconfigurable square into faces of hexahedron, RDHM based on 1-AE-EPaM can then be built. As shown in Fig. 6, the six basic configurations of RDHM correspond to the ones of 1-AE-EPaM in Fig. 5. The RDHM can switch to DSCM mode I and SSCM mode I from transition configuration I, and switch to DSCM mode II and SSCM mode II from transition configuration II. The RDHM also can switch between transition configuration I and transition configuration II.

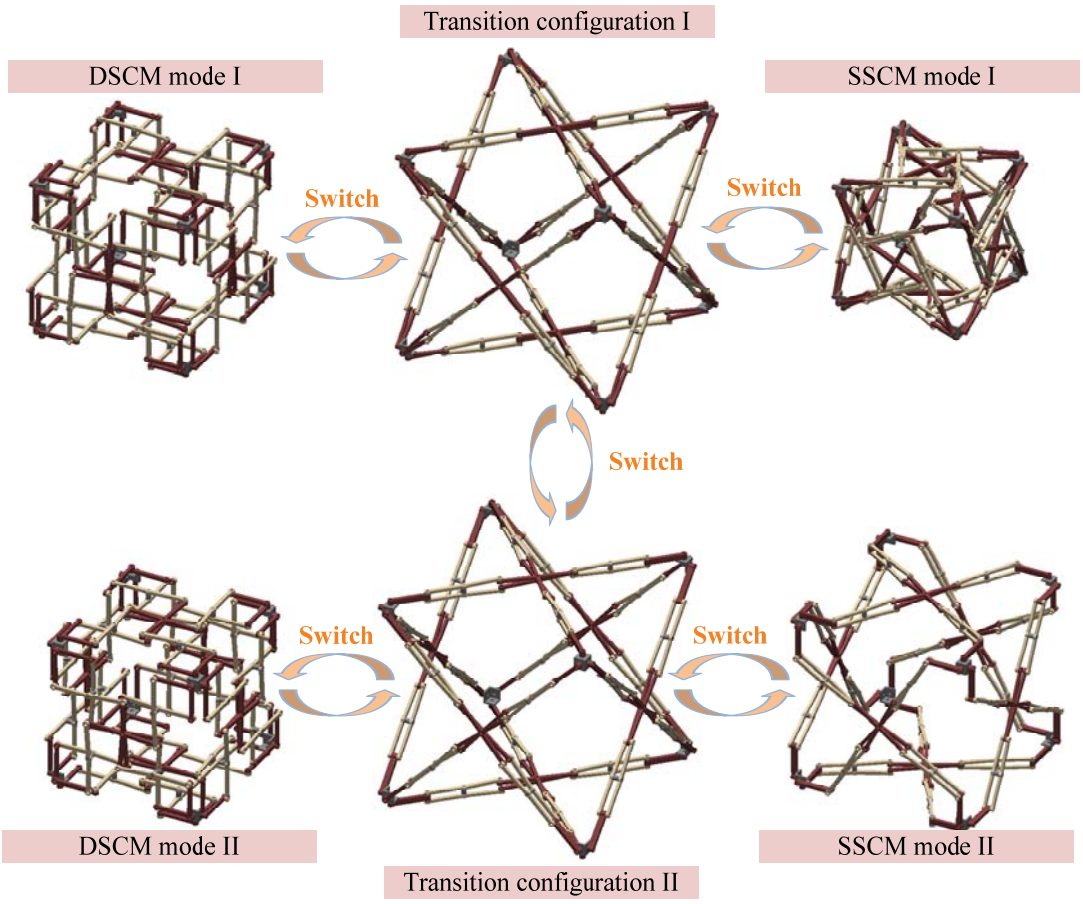

Fig. 6 Reconfigurable deployable hexahedral mechanism based on 1-AE-EPaM.

3.2 2-AEs-EPaM

The length difference between the crank and the link of 1-AE-EPaM in the SSCM mode is relatively large. To reduce the difference between the crank and the link in the SSCM mode, EPaMs with two AEs (2-AEs-EPaM) will be used. As shown in Fig. 7, a 2-AEs-EPaM consists of two central links, two edge links and two pairs of AEs. To let joints F and G coincide, $\angle ASB$ must be larger than $\angle FSG$ and $\angle CS'D$ must be larger than $\angle FS'G$. One feasible structure design is shown in Fig. 7(b). In the transition configuration (Fig. 8(a)), joints F and G coincide, and both $\angle FSG$ and $\angle FS'G$ decrease to zero. The distance between any two adjacent revolute joints is denoted by L. The diameter of revolute joints is denoted by w. Let joints A and B, C and D be tangent to each other when joints F and G coincide. The included angles γ_1 and γ_2 of AE-1 and AE-2 can still be calculated by $\pi-\arcsin(w/2L)$ and uniformly represented by γ.

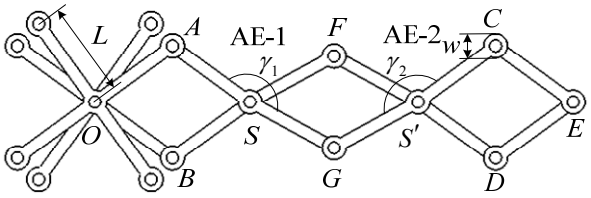

(a)

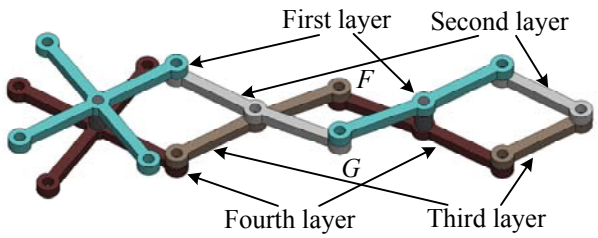

(b)

Fig. 7 2-AEs-EPaM: (a) Schematic diagram of 2-AEs-EPaM in DSCM mode, (b) structure design.

In the transition configuration, joints *F* and *G* merger into one common joint. In the SSCM mode (Fig. 8(b)), point *O* is fixed to virtual axis *OE*, crank *OG* rotates around point *O* and point *E* will slide along virtual axis *OE*. Figure 9 shows an RDHM constructed by 2-AEs-EPaM.

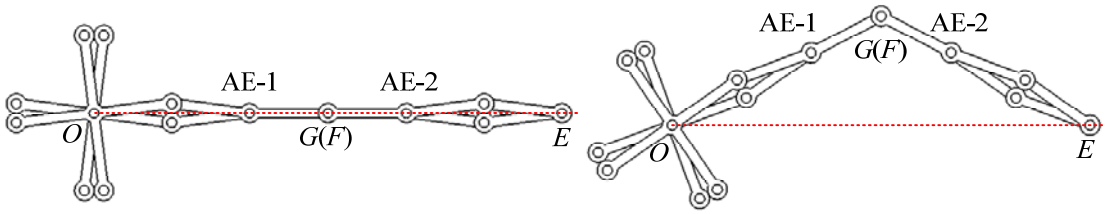

(a) (b)

Fig. 8 2-AEs-EPaM: (a) Transition configuration, (b) SSCM mode.

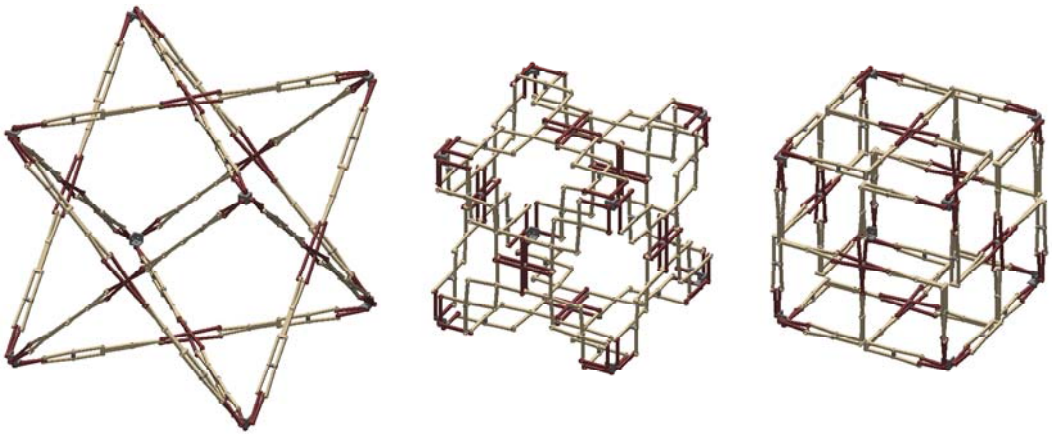

(a) (b) (c)

Fig. 9 Reconfigurable deployable hexahedral mechanism based on 2-AEs-EPaM: (a) Transition configuration, (b) DSCM mode, (c) SSCM mode.

A 2-AEs-EPaM with SEs (2-AEs-*m*-*n*-SEs-EPaM) can also be constructed by inserting *m* pairs of SEs at points *A* and *B* and *n* pairs of SEs at points *C* and *D*, as shown in Fig. 10(a). The 2-AEs-*m*-*n*-SEs-EPaM reaches its transition configuration (Fig. 10(b)) when joints *F* and *G* coincide with each other. The mechanism in the SSCM mode is shown in Fig. 10(c).

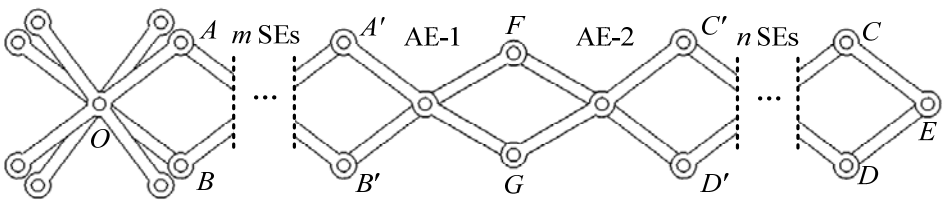

(a)

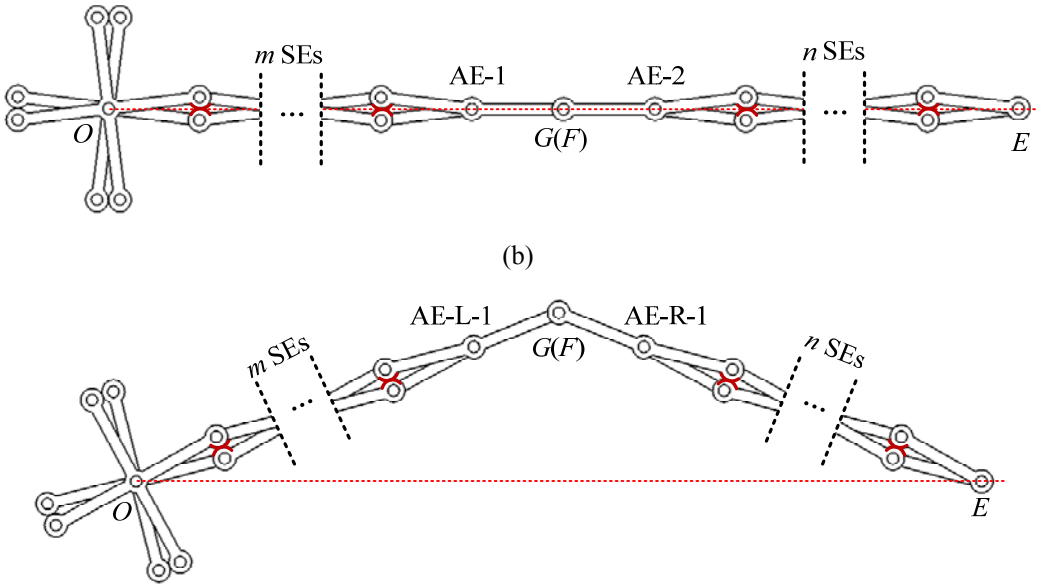

Fig. 10 2-AEs-*m*-*n*-SEs-EPaM: (a) DSCM mode, (b) transition configuration, (c) SSCM mode.

The magnification ratio of RDPM, which can be calculated by the magnification ratio of reconfigurable polyhedral face, can further be calculated by 2-AEs-*m*-*n*-SEs-EPaM. It is worth noting that 2-AEs-*m*-*n*-SEs-EPaM cannot deploy beyond the boundaries of the constructed polygon in order to avoid interference between two adjacent faces of RDPM. The magnification ratio of the polyhedral face constructed by 2-AEs-*m*-*n*-SEs-EPaM in the DSCM mode can be calculated by:

$$\mathrm{R}_{\mathrm{Dm}}=\frac{OE_{\max}}{OE_{\mathrm{Dmin}}} \tag{3}$$

where $OE_{\max}$ denotes the maximum distance between points O and E in Fig. 10(b), and OE_{Dmin} denotes the minimum distance between points O and E in the DSCM mode.

The magnification ratio of the polyhedral face constructed by 2-AEs-*m*-*n*-SEs-EPaM in the SSCM mode can be calculated by:

$$\mathrm{R}_{\mathrm{Sm}}=\frac{OE_{\max}}{OE_{\mathrm{Smin}}} \tag{4}$$

where $OE_{\max}$ denotes the maximum distance between points O and E in Fig. 10(b), and OE_{Smin} denotes the minimum distance between points O and E in the SSCM mode.

The maximum distance ($OE_{\max}$) between points O and E occurs when 2-AEs-*m*-*n*-SEs-EPaM is in its transition configuration (Fig. 10(b)), and it can be calculated by:

$$OE_{\max}=OG_{\max}+GE_{\max}=2L+2(m+n+2)L\cos(\pi-\gamma) \tag{5}$$

where $\gamma=\pi-\arcsin(w/2L)$, $OG_{\max}=L+2(m+1)L\cos(\pi-\gamma)$, $GE_{\max}=L+2(n+1)L\cos(\pi-\gamma)$.

The minimum distance (OE_{Dmin}) between points O and E in the DSCM mode occurs when $\angle CED$ in Fig. 10(a) turns to the interior angle of the polygon.

$$OE_{\mathrm{Dmin}}=2(m+n+2)L\cos\frac{\theta}{2}+2L\cos(\frac{\theta}{2}+\gamma-\pi) \tag{6}$$

where θ denotes the interior angle of the polygon constructed by 2-AEs-*m*-*n*-SEs-EPaM.

OE_{Smin} can be calculated in three cases. If $m>n$, the maximum length ($OG_{\max}$) of crank OG is greater than the maximum length ($GE_{\max}$) of link GE. The minimum distance (OE_{Smin}) between points

O and E in the SSCM mode occurs when $\angle OEG$ turns to $\theta/2$. $\angle GOE$ can be obtained by:

$$\sin\angle GOE = \frac{EG_{\max}}{OG_{\max}}\sin\frac{\theta}{2} \tag{7}$$

OE_{Smin} can be calculated by:

$$OE_{\mathrm{Smin}} = \sqrt{OG_{\max}{}^2 + GE_{\max}{}^2 - 2OG_{\max}\times GE_{\max}\cos\angle OGE} \tag{8}$$

where $\angle OGE = \pi - \angle GOE - \angle OEG$.

If $m=n$, $OG_{\max}$ is equal to $GE_{\max}$. The minimum distance (OE_{Smin}) between points O and E in the SSCM mode occurs when $\angle OEG$ turns to $\theta/2$.

$$OE_{\mathrm{Smin}} = 2OG_{\max}\cos\frac{\theta}{2} \tag{9}$$

If $m<n$, $OG_{\max}$ is less than $GE_{\max}$. The minimum distance (OE_{Smin}) between points O and E in the SSCM mode occurs when $\angle OGE$ turns to $\theta/2$.

$$OE_{\mathrm{Smin}} = \sqrt{OG_{\max}{}^2 + GE_{\max}{}^2 - 2OG_{\max}\times GE_{\max}\cos\frac{\theta}{2}} \tag{10}$$

4 Reconfigurable deployable polyhedral mechanism based on EPaM

The RDPMs can be constructed using EPaMs in three steps:

Step 1: Design the polyhedral faces using EPaMs.

Step 2: Insert the transition configuration of polyhedral faces into base polyhedron.

Step 3: Connect the polyhedral faces with edge connectors.

Theoretically, polyhedra with regular polygons (Platonic polyhedra, semiregular polyhedra and Johnson polyhedra) can be used as base polyhedra to construct RDPMs. In the following, the synthesis of the RDPMs based on 2-AEs-EPaMs will be discussed in detail. This method can be easily extended to RDPMs based on other EPaMs.

As shown in Figs. 11-13, triangle, pentagon and hexagon can be constructed by using three, five, and six 2-AEs-EPaMs, respectively. For Step 1, the key to design the polyhedral faces is to identify the parameters of 2-AEs-EPaMs. Let l denote the side length of a polygon constructed by 2-AEs-EPaMs. The maximum value of l ($l_{\max}$) can be written as follows:

$$l_{\max}^2 = OE_{\max}^2 + OE_{\max}^2 - 2OE_{\max}^2\cos(\pi-\theta) \tag{11}$$

where θ denotes the interior angle of the polygon constructed by 2-AEs-EPaMs. $OE_{\max}$ can be calculated by Eq. (5).

Let l_i and l_j denote the side length of two adjacent polygonal faces of base polyhedron. In order to merger the edge of two adjacent polygonal faces, l_i and l_j must have the same maximum value.

$$l_{i\max} = l_{j\max} \tag{12}$$

Substituting Eq. (11) into Eq. (12), we obtain the constraint equation for the parameters of two adjacent polygonal faces as follows

$$\frac{OE_{i\max}}{OE_{j\max}} = \sqrt{\frac{1-\cos(\pi-\theta_j)}{1-\cos(\pi-\theta_i)}} \tag{13}$$

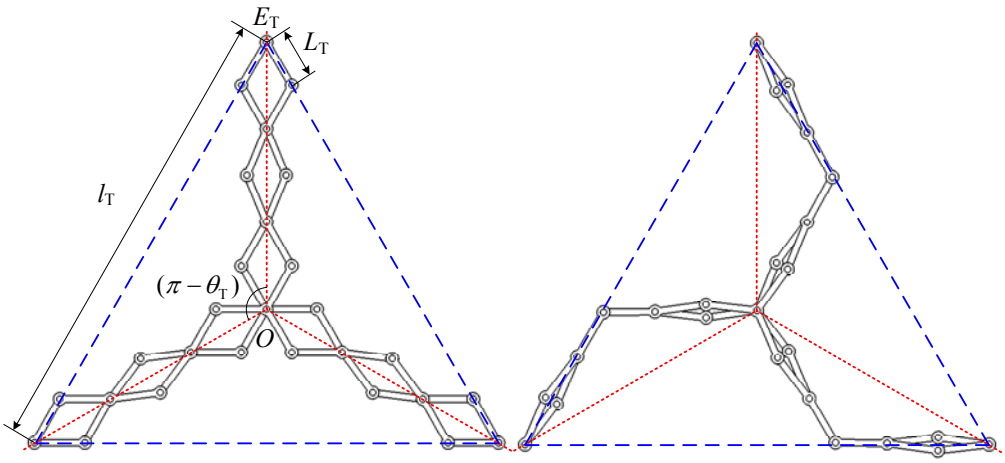

Fig. 11 Triangle constructed by three 2-AEs-EPaMs: (a) DSCM mode, (b) SSDM mode.

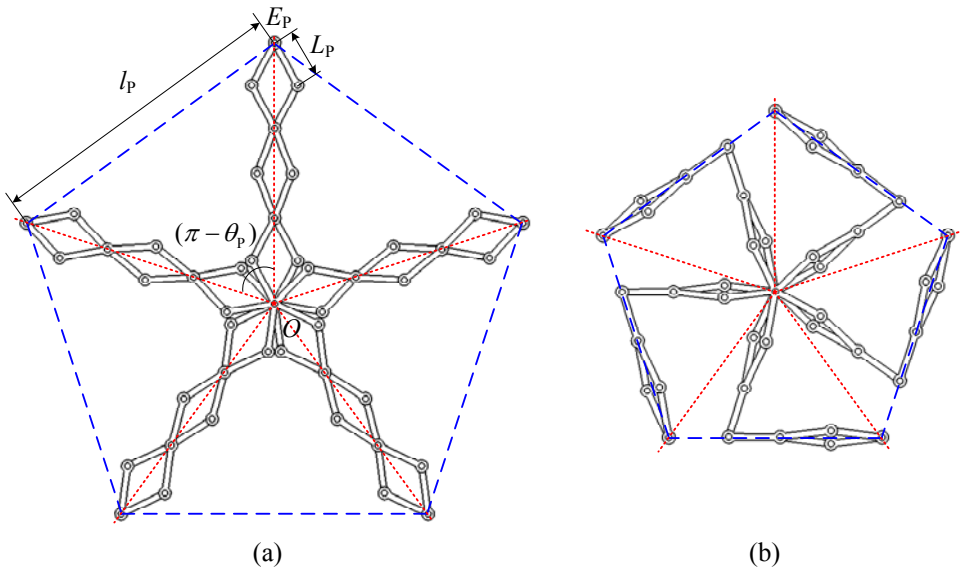

Fig. 12 Pentagon constructed by five 2-AEs-EPaMs: (a) DSCM mode, (b) SSDM mode.

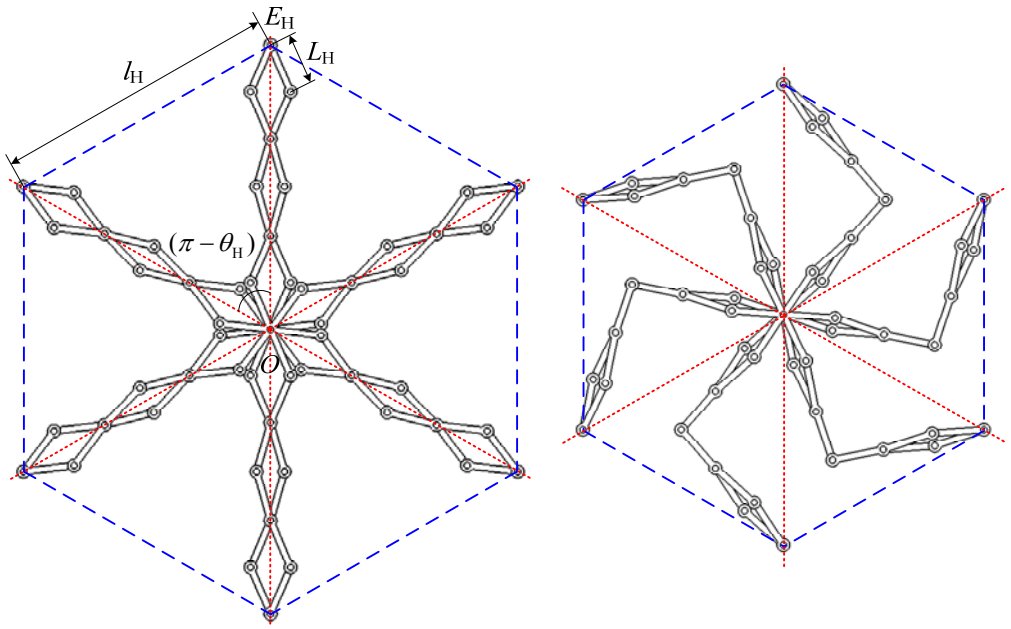

Fig. 13 Hexagon constructed by six 2-AEs-EPaMs: (a) DSCM mode, (b) SSDM mode.

Step 3 is to connect the adjacent polygonal faces. The RDPM based on hexagonal prism is used as an example to illustrate the construction process. To connect the adjacent polygonal faces, an edge connector (Fig. 14(b)) with three axes (axes 1, axes 2 and axes 3) is designed. Three axes intersect at one common point. For the edge connector of RDPM based on hexagonal prism, included angles between axes 1 and axes 2, axes 1 and axes 3, axes 2 and axes 3 are 90 degrees, 90 degrees, 60 degrees, respectively. The link length and joint diameter of hexagonal face are denoted by L_H and w_H, and the link length and joint diameter of quadrilateral face are denoted by L_Q and w_Q. Let w_H=w_P=10 mm and L_Q=40 mm, then L_H can be calculated using Eqs. (5) and (13) and is equal to 56.42 mm. The side lengths of quadrilateral face and hexagonal face are the same and equal to 337.64 mm. The constructed RDPM based on hexagonal prism consists of two hexagonal faces and six square faces, and all faces reach their transition configurations at the same time, as shown in Fig. 15.

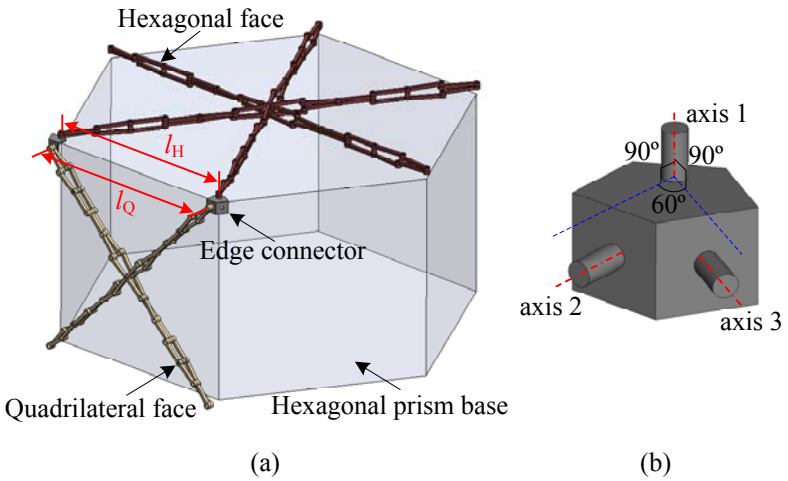

Fig. 14 RDPM based on hexagonal prism: (a) Construction process, (b) edge connector.

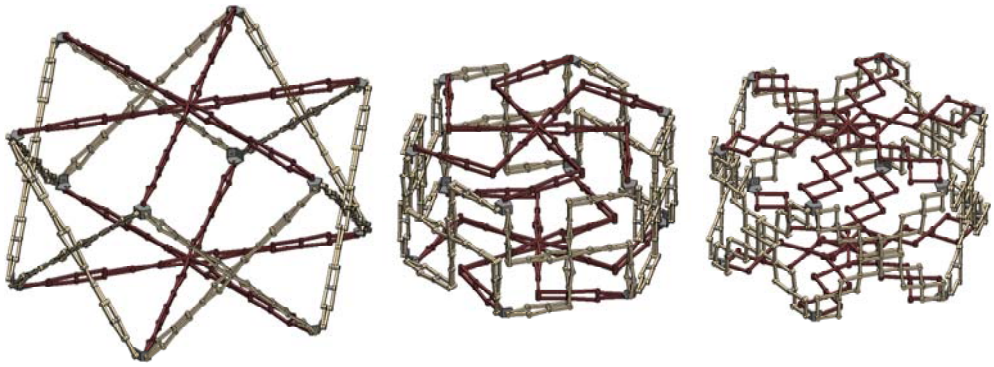

(a) (b) (c)

Fig. 15 RDPM based on hexagonal prism: (a) Transition configuration, (b) SSCM mode, (c) DSCM mode.

Using the above-mentioned method, RDPMs based on truncated icosahedron can also be built, as shown in Fig. 16. The RDPM based on truncated icosahedron consists of 12 pentagonal faces and 20 hexagonal faces, and all faces reach their transition configuration at the same time. The parameters and magnification ratios of RDPMs based on hexagonal prism and truncated icosahedron are calculated and listed in Table 1, where L_{H}, L_{Q} and L_{P} represent the link lengths of hexagon, pentagon and quadrilateral, w_{H}, w_{Q} and w_{P} represent the diameters of revolute joints of hexagon, pentagon and quadrilateral.

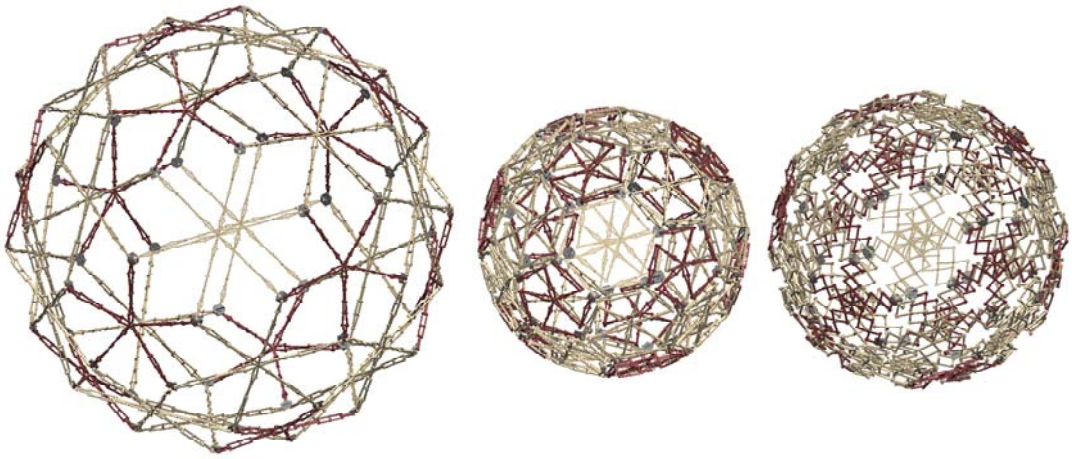

(a) (b) (c)

Fig. 16 RDPM based on truncated icosahedron: (a) Transition configuration, (b) SSCM mode, (c) DSCM mode.

In the following, the RDPM based on truncated icosahedron in Fig. 16 is used to study the magnification ratio with respect to link length and joint diameter. Assume that the link length of hexagonal face (L_{H}), joint diameter of hexagonal face (w_{H}) and joint diameter of pentagonal face (w_{P}) are given, and w_{H}=w_{P}, then L_{P} can be calculated using Eqs. (5) and (13). Furthermore, the magnification ratios of pentagonal face in SSCM mode ($\mathrm{R}_{\mathrm{Sm}}^{P}$) and DSCM mode ($\mathrm{R}_{\mathrm{Dm}}^{P}$) and the magnification ratios of hexagonal face in SSCM mode ($\mathrm{R}_{\mathrm{Sm}}^{H}$) and DSCM mode ($\mathrm{R}_{\mathrm{Dm}}^{H}$) can be calculated separately. The overall magnification ratios of RDPMs in SSCM mode ($\mathrm{R}_{\mathrm{Sm}}^{O}$) and DSCM mode ($\mathrm{R}_{\mathrm{Dm}}^{O}$) can be calculated using Eqs. (14) and (15), respectively.

$$\mathrm{R}_{\mathrm{Sm}}^{O}=\min\{\mathrm{R}_{\mathrm{Sm}}^{P},\mathrm{R}_{\mathrm{Sm}}^{H}\} \tag{14}$$

$$R_{Dm}^{O}=\min\{R_{Dm}^{P}, R_{Dm}^{H}\} \tag{15}$$

For the pentagonal face and hexagonal face, R_{Sm}^{P} and R_{Sm}^{H} are equal to $1/\cos(\pi/3)$ and $1/\cos(3\pi/10)$, respectively. So R_{Sm}^{O} is constant and equals to $1/\cos(3\pi/10)$. Figure 17 shows the mesh grids of R_{Dm}^{O} and w_H/L_H with respect to L_H and w_H. R_{Dm}^{O} increases with the decrease of w_H/L_H.

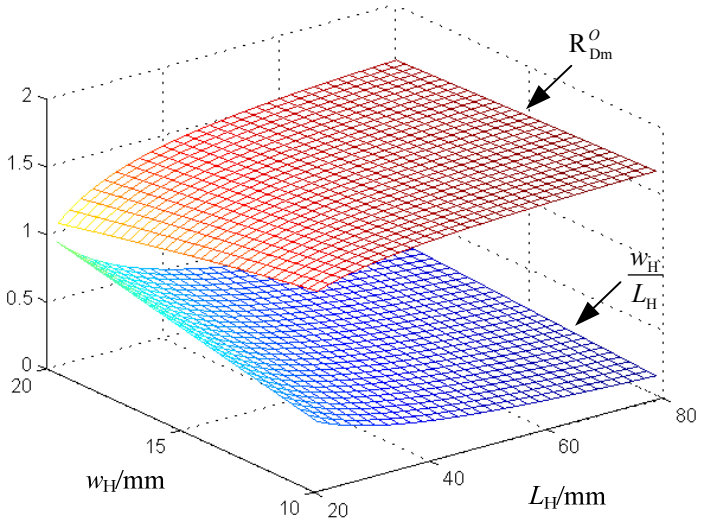

Fig. 17 Mesh grids of R_{Dm}^{O} and w_H/L_H with respect to L_H and w_H

Table 1

Parameters of RDPMs based on hexagonal prism and truncated icosahedron.

RDHMs based on	Number of link/element			Size parameters					R_m^O	
	Central link	Edge link	AE	L_H/mm	L_Q/mm	L_P/mm	$w_H=w_Q=w_P$ /mm	l_{max}/mm	R_{Sm}^{O}	R_{Dm}^{O}
hexagonal prism	16	72	72	56.42	/	40	10	332.34	1.41	1.33
truncated icosahedron	64	360	360	46.95	40	/	10	276.26	1.58	1.70

5 Prototype

A prototype of RDHM based on 2-AEs-EPaM was fabricated, as shown in Fig. 18. The distance between two adjacent revolute joints and the diameter of revolute joints were 60 mm and 10 mm, γ and l_{max} can be obtained by Eq. 2 and Eq. 11, respectively, furthermore the overall magnification ratios of RDPMs can be calculated by Eqs. 14 and 15. The parameters of RDHM based on 2-AEs-EPaM are listed in Table 2. This prototype of RDHM can be manually operated to switch between the SSCM mode and DSCM mode in the transition configuration. By removing some parts of this prototype, the other two RDHMs based on PaM and 1-AE-EPaM can be reassembled separately, as shown in Figs. 19 and 20. Since RDHM based on 1-AE-EPaM has two SSCM modes, its overall magnification ratio in SSCM mode can be calculated by finding its maximum configuration and minimum configuration in two SSCM modes. The detailed calculation is omitted due to space limitations. The parameters of RDHM based on PaM and 1-AE-EPaM are also listed in Table 2. Since the exiting hexahedral cupola [24] is a theoretical model without an actual magnification ratio, its ratio is approximately equal to the

ratio of RDHM based on PaM. In each mode, the overall magnification ratios of RDHM based on 1-AE-EPaM are greater than the ratios of the other two RDHMs. During the deployment in SSCM mode, side length range of RDHMs based on PaM, 1-AE-EPaM and 2-AEs-EPaM are [120.36 mm, 169.71 mm] and [202.59 mm, 338.32mm], [360.24 mm, 507.94 mm], respectively. When we have the prototype above-mentioned, we can assembly or reassembly the RDPMs to achieve huge size change beyond the deployment capacity. In addition, the testing of the prototype has shown that the more the basic elements are, the larger the assembly error is. The error analysis of RDPMs will be the focus of our future work.

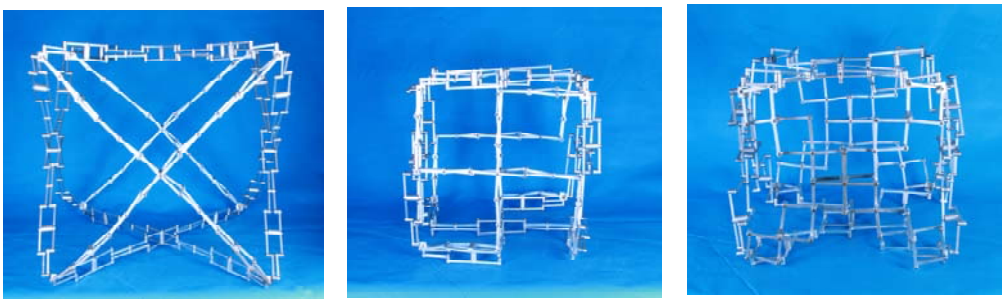

(a) (b) (c)

Fig. 18 Prototype of RDHM based on 2-AEs-EPaM: (a) Transition configuration, (b) SSCM mode, (c) DSCM mode

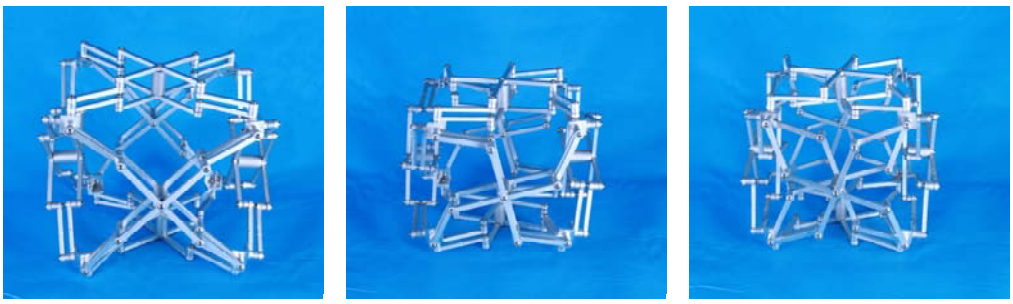

(a) (b) (c)

Fig. 19 Prototype of RDHM based on PaM: (a) Transition configuration, (b) SSCM mode, (c) DSCM mode

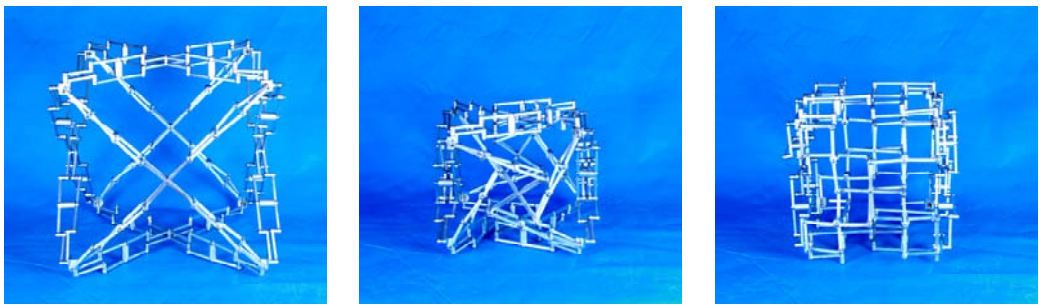

(a) (b) (c)

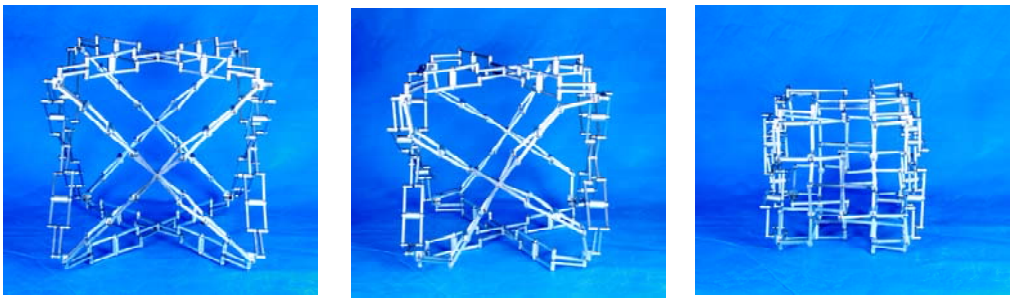

(e) (f) (g)

Fig. 20 Prototype of RDHM based on 1-AE-EPaM: (a) Transition configuration I, (b) SSCM mode I, (c) DSCM mode I, (e) transition configuration II, (f) SSCM mode II, (g) DSCM mode II.

Table 2

Parameters of three RDHMs.

Prototypes of RDHMs based on	Number of link/element			Size parameters				R_m^O	
	Central link	Edge link	AE	L/mm	w/mm	γ/degree	l_{max}/mm	R_{Sm}^O	R_{Dm}^O
PaM	12	48	0	60	10	175.22	169.71	1.41	1.41
1-AE-EPaM	12	48	24	60	10	175.22	338.32	1.67	1.48
2-AEs-EPaM	12	48	48	60	10	175.22	507.94	1.41	1.37

6 Conclusion

A method has been proposed to synthesize reconfigurable deployable polyhedral mechanisms (RDPMs) based on extended parallelogram mechanisms. 1-AEs-EPaM and 2-AEs-EPaM have been constructed with their parameter conditions identified. The calculation method of magnification ratios of RDPMs have been given by considering links' length and joints' size. RDPMs based on hexagonal prism and truncated icosahedron have been constructed as examples. RDHMs based on PaM, 1-AEs-EPaM and 2-AEs-EPaM have been constructed in 3D software and fabricated in reality. The proposed method provided more modular linkages for RDPMs and the obtained RDPMs can be reassembled into different sizes.

The study found that RDPM based on 1-AEs-EPaM had more motion modes and bigger magnification ratio and it was a qualified candidate to increase the adaptability of deployable mechanisms. The reassembled function of RDPMs can be used to meet a variety of application requirements, such as the size change beyond the deployment capacity of the RDPMs.

In the future, we would like to extend the work in two directions. First, we would like to optimize the parameters of the face and EPaMs according to RDPMs' magnification ratio and size. Second, we would like to carry out the error analysis of RDPMs by considering the gaps in the revolute joints.

Acknowledgement

This work was supported by the National "Climbing" Program of China (2015BAK04B02).

References

[1] Hanaor A, Levy R. Evaluation of deployable structures for space enclosures[J]. *Int J Space Struct*, 2001, 16(4): 211-229.

[2] Maden F, Korkmaz K, Akgün Y. A review of planar scissor structural mechanisms: geometric principles and design methods[J]. *Archit Sci Rev*, 2011, 54(3): 246-257.

[3] Pinero E P. Project for a mobile theatre[J]. *Archit Design*, 1961, 12(1): 154-155.

[4] Escrig F, Valcarcel J P. Geometry of expandable space structures[J]. *Int J Space Struct*, 1993, 8(1-2): 71-84.

[5] Zhao J S, Chu F, Feng Z J. The mechanism theory and application of deployable structures based on SLE. *Mech Mach Theory* 2009; 44(2): 324-335.

[6] Gantes C J, Konitopoulou E. Geometric design of arbitrarily curved bi-stable deployable arches with discrete joint size. *Int J Solids Struct* 2004; 41(20): 5517-5540.

[7] Ding X, Yang Y, Dai J S. Design and kinematic analysis of a novel prism deployable mechanism. *Mech Mach Theory* 2013; 63: 35-49.

[8] Hoberman C. Reversibly expandable doubly-curved truss structure. Patent 4,942,700, USA, 1990.

[9] You Z, Pellegrino S. Foldable bar structures. *Int J Solids Struct* 1997; 34(15): 1825-1847.

[10] Wohlhart K. Polyhedral zig-zag linkages. In: Lenarcic J and Galletti C (eds.) *On Advances in Robot Kinematics*. Springer Netherlands, 2004, pp. 351-360.

[11] Wohlhart K. Regular polyhedral linkages. 2nd Workshop on Computational Kinematics, Seoul, Korea, September 2001, pp. 4-6.

[12] Wohlhart K. Twisting towers derived from Archimedean polyhedrons. *Mech Mach Theory* 2014; 80: 103-111.

[13] Wei G, Chen Y, Dai J S. Synthesis, mobility, and multifurcation of deployable polyhedral mechanisms with radially reciprocating motion. *J Mech Des-T ASME* 2014; 136(9): 091003.

[14] Kiper G, Söylemez E, Kişisel A U Ö. A family of deployable polygons and polyhedral. *Mech Mach Theory* 2008; 43(5): 627-640.

[15] Kovács F, Tarnai T, Fowler P W, et al. Double–link expandohedra: a mechanical model for expansion of a virus. *P Roy Soc Lond A Mat* 2004; 460(2051): 3191-3202.

[16] Wei X Z, Yao Y A, Tian Y B, et al. A new method of creating expandable structure for spatial objects. *P I MECH ENG C-J MEC* 2006; 220(12): 1813-1818.

[17] Gosselin C M, Gagnon-Lachance D. Expandable polyhedral mechanisms based on polygonal one-degree-of-freedom faces. *P I MECH ENG C-J MEC* 2006; 220(7): 1011-1018.

[18] St-Onge D, Gosselin C. Synthesis and Design of a One Degree-of-Freedom Planar Deployable Mechanism With a Large Expansion Ratio. *J Mech Robot-T ASME* 2016; 8(2): 021025.

[19] Kong X. Reconfiguration analysis of a 3-DOF parallel mechanism using Euler parameter quaternions and algebraic geometry method. *Mech Mach Theory* 2014; 74: 188-201.

[20] Kong X, Jin Y. Type synthesis of 3-DOF multi-mode translational/spherical parallel mechanisms with lockable joints. *Mech Mach Theory* 2016; 96: 323-333.

[21] Wei G, Dai J S. Reconfigurable and deployable platonic mechanisms with a variable revolute joint. In: Lenarcic J and Khatib O (eds.) *Advances in Robot Kinematics*. Springer International Publishing, 2014, pp. 485-495.

[22] Li R, Yao Y, Kong X. A Method for Constructing Reconfigurable Deployable Polyhedral Mechanism. In: Ding X, Dai J and Kong X (eds.) *Advances in Reconfigurable Mechanisms and Robots II*. Springer International Publishing, 2016, pp. 1023-1035.

[23] Li R, Yao Y, Kong X. A class of reconfigurable deployable platonic mechanisms. *Mech Mach Theory*, 2016; 105: 409-427.
[24] Wohlhart K. Cupola linkages. In: *12th IFToMM World Congress*. Besançon, France, June 18-21 2007.